ELSEVIER

International Journal of Mass Spectrometry 202 (2000) 121–137

International Journal of Mass Spectrometry

Mass spectrometric study of the molecular and ionic sublimation of cesium iodide single crystals

M.F. Butman[a], L.S. Kudin[a], A.A. Smirnov[a], Z.A. Munir[b]

[a]*Department of Physics, State University of Chemical Sciences and Technology, Prosp. Engelsa 7, 153460 Ivanovo, Russian Federation*
[b]*Department of Chemical Engineering and Materials Science, University of California, Davis, CA 95616, USA*

Received 11 October 1999; accepted 7 March 2000

Abstract

A mass spectrometric method was used to study the thermodynamics and vaporization kinetics of cesium iodide single crystal. In electron-impact-ionization mass spectra of molecular fluxes effusing from Knudsen cell (case A) or vaporized from an open crystal surface (case B), ions of Cs^+, CsI^+, I^+, Cs_2I^+, and Cs_2^+ originating from CsI and Cs_2I_2 molecular precursors were detected in the temperature range 656–838 K. The temperature dependence of ion currents, $\ln(I_iT) - 1/T$, of the most abundant Cs^+, CsI^+, and Cs_2I^+ ions were measured in both cases. From the results of case A (Knudsen cell), the enthalpies of sublimation to monomers and dimers were determined as, Δ_sH^0(CsI, 736 K) = 170.9 ± 1.7 and Δ_sH^0(Cs_2I_2, 749 K) = 209.8 ± 3.2 kJ mol^{-1}, respectively. For case B, the temperature dependence exhibited a departure from the linearity. From a comparison between the equilibrium and nonequilibrium vaporization rates, it was concluded that the value of the vaporization coefficient passes through a maximum. A dimer-to-monomer ratio was found to increase with temperature at a continually increasing rate in case A, and at a rate passing through a maximum in case B. The electron-impact-fragmentation pattern of CsI molecules exhibited a roughly linear dependence on temperature in case A, but exhibited a minimum in case B. In the thermionic emission mass spectrum, the positive ions Cs^+, Cs_2I^+, $Cs_2I_2^+$, and Cs_2^+ were identified in the temperature range 600–890 K. The emission of I^- and CsI_2^- negative ions was detected only above approximately 850 K. It was found that in contrast to the molecular sublimation, the compositions of ion beams from the Knudsen cell and from the free crystal surface differ significantly. The temperature dependence $\ln I(Cs^+) - 1/T$, measured in the range 640–820 K, revealed a change in slope. The results are discussed in light of the terrace–ledge–kink and surface charge models. (Int J Mass Spectrom 202 (2000) 121–137) © 2000 Elsevier Science B.V.

Keywords: Cesium iodide; Alkali halides; Single crystal; Vaporization; Sublimation; Crystal defects; Thermionic emission; Mass spectrometry

1. Introduction

Vaporization from solids is of both theoretical and practical interest because of the importance of the process in the fabrication, application, or degradation of solid-state materials, especially at elevated temperatures. Morphological and defect-related surface properties of solids are of fundamental importance for understanding and simulating the vaporization kinetics [1]. The vaporization rate is influenced by many factors, including the various types of surface rearrangements during vaporization, concentration of impurities, and surface stoichiometry.

Modern insight into the vaporization mechanism stems basically from the terrace–ledge–kink (TLK)

* Corresponding author.

PII S1387-3806(00)00232-3

model [2]. According to this model the vaporization process incorporates three successive stages: (1) removal of atoms, ions or molecules from kinks and ledges; (2) diffusion and molecular association in the adsorbed layer; and (3) desorption. Additionally, in the case of ionic and semiconducting solids, the surface charge (electrical boundary layer), arising from differences in the Gibbs free energy of formation of intrinsic cation and anion vacancies or from extrinsic defects has been proposed as an important contributing factor to the vaporization [3–8]. Specifically, observations such as the anisotropic nature of the vaporization rate from different crystalline faces [9,10], the transient vaporization rate [6,8], the influence of impurities [11,12] and the field-enhanced/retarded vaporization [13–15] have been interpreted in terms of a surface charge model.

In general, the degree of retardation of free-surface vaporization of solids in comparison with equilibrium vaporization is characterized by a vaporization coefficient, α_v. It is defined as the ratio of the flux of molecules of a given species from freely vaporizing crystal surface to that from the crystal surface which is in equilibrium with a saturated vapor phase [1]. In accordance with the TLK model, the vaporization coefficient can be expressed as a product of parameters representing various constraints in the mechanism of vaporization [16], that is

$$\alpha_v = \alpha_e \alpha_d \alpha_l \cdots, \quad (1)$$

where α_e is an entropy-related factor, α_d is a surface-diffusion-related factor, and α_l is a factor representing ledge constraint. Each of these has limits between 0 and 1.

It has been demonstrated recently [17,18] that both the TLK model and the concept of surface charge are helpful to interpret the temperature variation in the vaporization coefficient observed in the cases of NaCl [19], KCl [17], and KBr [18] single-crystal vaporization. To further elucidate the vaporization kinetics of alkali halides, this work was undertaken to investigate the thermodynamics and kinetics of the sublimation of CsI single crystals by mass spectrometry. The investigation of free-surface vaporization integrally with Knudsen cell measurements is worthwhile to avoid the systematic instrumental error upon comparison of the equilibrium and nonequilibrium vaporization rates. Such an investigation would supplement the measurements of integral vaporization fluxes from an open CsI surface by a thermobalance [20] and of the molecule velocity distribution in such fluxes by a velocity selector coupled with a surface ionization detector [21]. The former method resulted in observation of a significant decrease in α_v with increasing temperature of solid CsI. From the analysis of the flux chemical composition by the latter technique it followed that no dimer species Cs_2I_2 sublime from an open surface of CsI, whereas the Knudsen cell mass spectrometric studies of saturated vapor composition of CsI demonstrated the presence of dimers [22–24]. Therefore, the results of both investigations [20,21] need verification through a mass-spectrometric examination.

Apart from theoretical interest, the characterization of CsI vaporization is of practical significance. Such knowledge is necessary to understand the problem of chemical attack of fuel cladding materials in nuclear reactors [25] and also to explain the release of cesium and iodine into the coolant of high temperature gas cooled reactors [26].

An additional purpose of this work was to study the ionic sublimation from CsI single-crystal surfaces since the phenomenon of thermal ion emission was found to provide complementary information about the sublimation mechanism [17,27,28], especially in the cases when the detection of both positive and negative ions is possible [17,27]. From this point of view, cesium iodide seemed best suited for such a study because it is the only alkali halide that was found to emit positive and negative ions in nearly equal proportions under the equilibrium conditions [29,30].

2. Experimental

Measurements were carried out with a single focusing magnetic-sector mass spectrometer, MI 1201 (200 mm radius of curvature, 90°), which was modi-

fied for high temperature studies. The instrument is described in more detail elsewhere [17] and thus only a brief description is given here. The furnace assembly consisted of a molybdenum Knudsen cell or a stainless steel crystal holder (for the free surface studies), a molybdenum resistance heater, tantalum radiation shielding, and a movable stainless steel shutter plate. The Knudsen cell had a knife-edged orifice of diameter 0.6 mm and effusion-to-evaporation ratio less than 4×10^{-4}. In the case of Knudsen cell measurements the thermocouple was inserted into the bottom of the cell. In the case of free-vaporization measurements the thermocouple was held tightly between the crystal and the holder. Heating was controlled to provide temperatures with a maximum variation of ± 0.5 K. The shuttering of the vaporizing fluxes was used to distinguish ions formed by electron bombardment of neutral species vaporized from the cell or from the crystal surface from those formed by electron bombardment of residual background gas. The electron-impact-ionization mass spectra were recorded with an electron emission current of 1 mA and an electron energy of 70 eV. In the case of ionic sublimation measurements, the ions emitted were extracted by a weak electric field (the field strength was no higher than 5×10^4 V m^{-1}) applied between the crystal surface and the extracting electrode with an orifice of diameter 1 mm. In order to measure the emission of charged particles of both signs, the holder itself could be biased either positively or negatively with respect to ground. The ions produced via electron impact in the case of molecular sublimation or extracted from the crystal surface in the case of ionic sublimation were accelerated in an electrostatic field to energy of 3 keV, mass analyzed in a variable magnetic field, and collected on the first plate of an electron multiplier. The output from the multiplier was amplified by an electrometer utilizing 100 MΩ resistor and recorded. The sensitivity of the registration system was as high as 10^{-17} A.

In this work the samples to be vaporized were taken from high-purity commercial CsI single crystals (optical lens material). Because CsI crystals do not cleave, the samples to be vaporized in the case of free vaporization were cut by lancet. The orientation of the crystalline faces was not specified since it was shown by Ewing and Stern [20] that the free-vaporization rates of CsI are independent of orientation. The samples were maintained for several hours at about 450 K under low vacuum (10^{-1} Pa) prior to being heated up to the test temperatures.

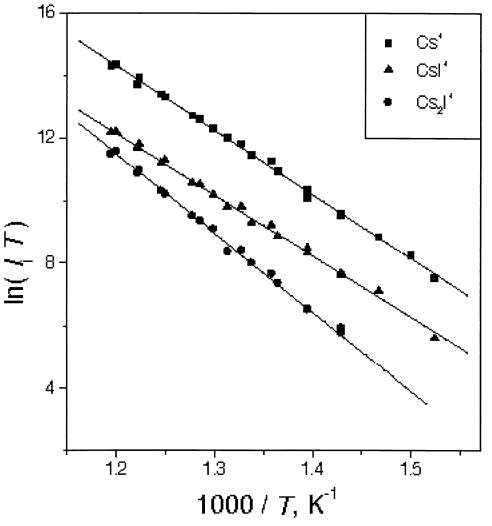

Fig. 1. Temperature dependence of ion currents (arbitrary units) in electron-impact-ionization mass spectrum of molecular fluxes effused from the Knudsen cell containing CsI.

3. Results and discussion

3.1. Molecular sublimination

3.1.1. Knudsen cell measurements

In the electron-impact-ionization mass spectrum of molecular fluxes effusing from the Knudsen cell, the ions Cs^+ (100), CsI^+ (15.9), I^+ (10.5), Cs_2I^+ (5.6), and Cs_2^+ (0.7) were identified. The typical values of the relative ion current intensities at 832 K are given in the parentheses. To obtain enthalpies of sublimation to monomers, $\Delta_s H^0$(CsI), and to dimers, $\Delta_s H^0(Cs_2I_2)$, the temperature dependence of the currents, I, of Cs^+, CsI^+, and Cs_2I^+ ions was measured over the interval 656–838 K in two successive heating and cooling procedures. These data are presented in Fig. 1, as $\ln(I_i T)$ versus $1/T$. The tempera-

ture dependence of I^+ and Cs_2^+ ion currents was not investigated since the high background at the mass 127 made it difficult to distinguish small shutter effects at temperatures below 800 K in the former case, and because of low intensity of ion current in the latter case. Based on the analysis of the ion appearance energies [24], the apparent sublimation enthalpies [24], and the results obtained by the double-cell distribution technique [22,23], it has been established that Cs^+, CsI^+, and I^+ ions originate exclusively from monomers (CsI), whereas Cs_2I^+ and Cs_2^+ ions are formed from dimers (Cs_2I_2). Since current intensities of I^+ and Cs_2^+ ions were low in comparison with those of Cs^+ and Cs_2I^+ ions, respectively, their disregard would not introduce significant error in the calculated sublimation enthalpies. The values $\Delta_s H^0$(CsI, 736 K) = 170.9 ± 1.7 kJ mol^{-1} and $\Delta_s H^0$(Cs_2I_2, 749 K) = 209.8 ± 3.2 kJ mol^{-1} were calculated from the respective slopes of the plots ln{[$I(Cs^+)$ + $I(CsI^+)$]T} versus $1/T$ and ln[$I(Cs_2I^+)T$] versus $1/T$, respectively. These values are in good agreement with $\Delta_s H^0$(CsI, 733 K) = 176.8 ± 1.8* kJ mol^{-1} [24], $\Delta_s H^0$(CsI, 800 K) = 163.3 ± 8.4 kJ mol^{-1} [31], $\Delta_s H^0$(CsI, 800 K) = 165.0 ± 2.1 kJ mol^{-1} [32], and $\Delta_s H^0$(Cs_2I_2, 733 K) = 209.5 ± 4.5[1] kJ mol^{-1} [24] obtained by the mass-spectrometric method.

3.1.2. Free-surface measurements

As in the case of Knudsen cell measurements, molecular fluxes from a freely vaporizing CsI surface contained, Cs^+ (100), CsI^+ (14.5), I^+ (9.8), Cs_2I^+ (5.3), and Cs_2^+ (0.06) ions. Their relative current intensities (shown within the parentheses at T = 820 K) are close to those in the effusion experiment with the exception of Cs_2^+. This observation is in contrast to the conclusion of Rothberg et al. [21] that the flux from a CsI single crystal surface consists of monomers only. Such a conclusion may stem from an invalid assumption on the relative detection efficiency of monomers and dimers and also, to a greater extent, from the reported distortion of the velocity distribution because of beam scattering [20].

* Calculated by us for the temperature range 654–833 K, using the original data from [24].

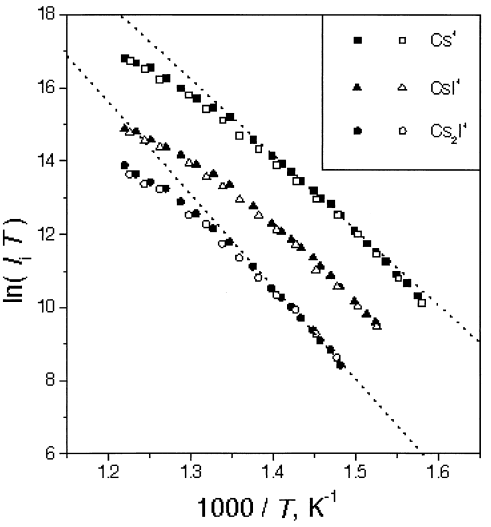

Fig. 2. Temperature dependence of ion currents (arbitrary units) in electron-impact-ionization mass spectrum of molecular fluxes vaporized from free surface of a CsI single crystal. Closed and open symbols correspond to the heating and cooling runs, respectively. Dotted lines are drawn as tangents with a slope equal to $-\Delta_s H(\mathrm{CsI})/R$ and $-\Delta_s H(Cs_2I_2)/R$, respectively.

The temperature dependence of Cs^+, CsI^+, and Cs_2I^+ ion currents measured in the free surface vaporization in the range 619–820 K is shown in Fig. 2. The reproducibility of the current intensities in the heating and cooling runs (solid and open points, respectively) is good, exhibiting only a small hysteresis. With reference to these results, it should be noted that prior to the current measurements the sample was heated to about 850 K and kept at this temperature for about 20 min, resulting in the removal of approximately 500 monolayers. This was done for two reasons. First, such an overheating was necessary to promote the development of a surface morphology that goes through the formation of etch pits (nucleated at points of dislocation emergence or by impurities [33]) and through probable formation of (110) faces, which seem to be the F faces in the case of CsI. Second, high temperature was favorable to the outgassing of the parts of furnace assembly in order to keep the vacuum at the same level in the course of measurements in the overall temperature interval. On the other hand, the overheating led to such a degree of

surface roughening which would be only little affected by further temperature variations.

One can see in Fig. 2 that, in contrast to the Knudsen cell measurements (Fig. 1), the temperature dependences of ion currents in the case of free-surface vaporization exhibit distinct curvature, as was observed in the cases of NaCl [19], KCl [17], and KBr [18] single-crystal vaporization. This implies that the value of the vaporization coefficient is temperature dependent. However, one may also suppose that the deviation of the dependencies from linearity could be produced by a rate-controlling heat-transfer process. Since vaporization is an endothermic process, significant self-cooling of the vaporization surface may lead to a retardation of the vaporization rate at high temperatures. To clarify this situation, calculations by Lester [34] of the heat balance on a heated alkali halide surface have been made to determine the maximum temperature gradient between the vaporizing surface and the crystal bulk. It was found that, for the rates of vaporization up to 0.1 mg cm^{-2} s^{-1} the heat flux to the sample surface could easily offset the heat loss due to vaporization. Thus, theoretically surface cooling should be negligible at the experimental vaporization rates and the surface temperature should be within 1° of the bulk temperature. Experimentally this was verified by Ewing and Stern [20]. These authors studied the isothermal (780°C) vaporization rates of NaCl crystals as a function of crystal lengths, diameters and shapes. They concluded that conduction through the crystal is the dominant mechanism of heat transfer and the absence of any change in rate with length or diameter precludes any self-cooling of the heat-transfer surface or rate control by a heat-transfer process. Therefore, we believe the temperature dependence of the vaporization coefficient observed by us and by Ewing and Stern [20], is not an experimental artifact.

The mass-spectrometric method does not provide for the determination of the absolute values of the vaporization coefficient. This is because it is difficult to specify the ratio of instrumental sensitivity constants for the cases of the Knudsen cell and free-surface measurements. Nonetheless, in order to elucidate the character of temperate dependence of α_v we have applied the procedure of data treatment proposed by us earlier [17,18]. Let δ be the factor that accounts for the departure of the experimental data in Fig. 2 from the linear behavior observed in the case of equilibrium vaporization (Fig. 1). Physically, δ has a significance of a temperature-dependent constituent of the vaporization coefficient. This factor can be determined as follows. The data of the dependence for Cs^+ and Cs_2I^+ in Fig. 2 were approximated by a third-order polynomial equations of the following forms:

$$\ln[I(Cs^+)T] = -87.6 + 233.4 \times 10^3(1/T) - 164.0 \times 10^6(1/T)^2 + 35.2 \times 10^9(1/T)^3 \quad (2)$$

$$\ln[I(Cs_2I^+)T] = -146.7 + 357.3 \times 10^3(1/T) - 253.1 \times 10^6(1/T)^2 + 55.8 \times 10^9(1/T)^3 \quad (3)$$

Eqs. (2) and (3), which refer to the cases of sublimation to monomers[†] and dimers, respectively, were used in each case to draw in Fig. 2 the lines that can be seen as tangents to the curves $\ln[I(Cs^+)T]$ versus $1/T$ and $\ln[I(Cs_2I^+)T]$ versus $1/T$ with slopes equal to $-\Delta_s H^0(CsI)/R$ (where R is the gas constant) and $-\Delta_s H^0(Cs_2I_2)/R$, respectively. The tangent-point temperatures were determined by setting the derivatives, $d[\ln(I_i T)]/d(1/T)$, equal to $-\Delta_s H^0(CsI)/R$ and $-\Delta_s H^0(Cs_2I_2)/R$, respectively. The values of δ were calculated as an exponential factor $\exp(-\Delta)$, where Δ is the difference between the magnitudes of the tangent and data points in Fig. 2 at each temperature. The results of such calculations are shown in Fig. 3. It can be seen from Fig. 3 that (1) the departure factor δ varies with temperature in a similar way for the monomer and dimer cases, (2) both temperature dependences of $\delta(Cs^+)$ and of $\delta(Cs_2I^+)$ have a maximum. With regard to the latter, its significance depends on the reliability of the low temperature measurements: the lower is the temperature, the larger

[†] In this treatment procedure the contribution of low-intensity CsI^+ ions is neglected.

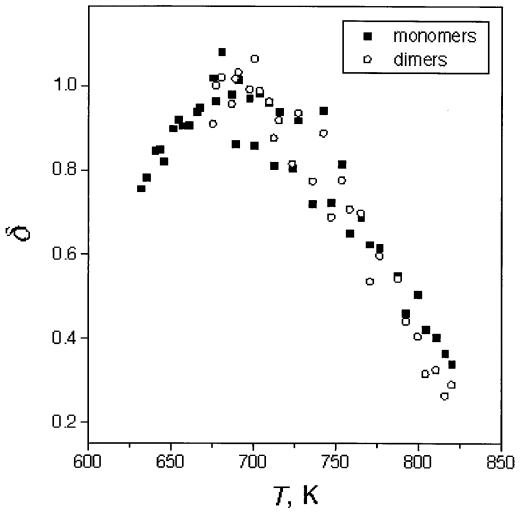

Fig. 3. Temperature dependence of the departure factor, δ.

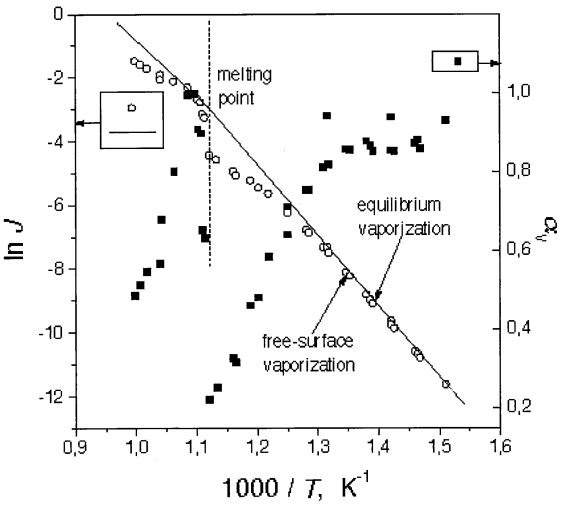

Fig. 4. Temperature dependence of the integral vaporization rate of CsI, J (kg m^{-2} s^{-1}), and the vaporization coefficient, α_v, as reported by Ewing and Stern [20].

are the errors of the individual points. To ensure sufficient reliability, the ion currents were measured in a temperature interval well above the detection limit. The lowest temperatures were set by a noise-to-signal ratio no higher than 20%. This condition would introduce an uncertainty of about 10% in ion current intensities and hence in the values of δ at the lowest temperatures.

It is interesting to compare our mass-spectrometric results with those obtained by Ewing and Stern using a thermobalance technique [20]. These authors measured the vacuum vaporization rate of CsI over a very wide temperature range, including temperatures above the melting point of this compound. The most interesting observation of this work [20] is that the vaporization coefficient is anomalously low just below the melting point of CsI but it rises rapidly just above the melting point, as seen in Fig. 4. Although the highest temperatures of our experiment are well below the melting point, our results show a change as we approach this temperature. The slope of ln J versus $1/T$ (where J is the molecular flux) at lower temperatures is constant but decreases progressively as the melting point is approached. However, in the work of Ewing and Stern [20] no deviations between free surface and equilibrium vaporization at lower temperatures were found. Their interpretation of the vaporization mechanism in terms of a simple two-step mechanism (a bulk-to-surface step followed by a desorption step) is inadequate because the first step is not expected to control the vaporization rate of molecular species [35].

3.1.3. TLK model analysis

From the standpoint of the TLK model there may be a number of different reasons for the departure of the dependence ln $J - 1/T$ from linearity in the case of free-surface vaporization. The decrease of the experimental α_v values with increasing temperature [in our case the high-temperature part of the $\delta(T)$ dependence] seems, at first consideration, to be caused by a decrease in the mean self-diffusion length, d, according to the following [2]:

$$d = r \exp[(E_{\mathrm{des}} - E_{\mathrm{diff}})/2kT] \quad (4)$$

where r is the jump distance of surface diffusion; E_{des} and E_{diff} are the activation energies for desorption and surface diffusion, respectively, and k is Boltzmann constant. The associated decrease of the constraint parameter α_d follows from the following relationship [35]:

$$\alpha_d = (d/\lambda)\ \tanh(\lambda/d) \quad (5)$$

where λ is the mean step separation.

To determine whether the parameter α_d alone can explain satisfactorily the decrease of the vaporization coefficient of alkali halides with increasing temperature, we have performed the following estimations. From definition of δ it follows that

$$\alpha_v(T_2)/\alpha_v(T_1) = \delta(T_2)/\delta(T_1) \quad (6)$$

Hence the experimental ratio $\delta(T_2)/\delta(T_1)$ should be compared to the estimated ratio $\alpha_d(T_2)/\alpha_d(T_1)$. Such a comparison is possible only in the case of KCl because, to our knowledge, it is the only alkali halide for which the saddle point energy, $E_{\text{des}} - E_{\text{diff}}$, was determined experimentally (0.82 ± 0.08 eV) [36]. This makes possible the calculation of d by Eq. (4), with the parameter r taken to be equal to the lattice constant ($r = 0.3145$ nm [37]). Besides, the calculation of α_d by Eq. (5) requires knowledge of λ. Here it is appropriate to once again note that in our experiments we start with a very rough surface after a fairly long period of vaporization at high temperatures. As a matter of experience, such a roughening is more or less irreversible. So, the value of λ is only slightly affected by further temperature variation and may be assumed approximately constant. The parameter λ can be derived directly from the studies of surface morphology by electron microscopic decoration technique. As far as we know, no such studies have been carried out for alkali halides at the temperatures higher than 700 K. From consistent results obtained with this technique by Munir et al. [38] (NaCl single-crystal studies) and by Dabringhaus and Meyer [39] (studies of thick NaCl overlayers on KCl) in the temperature range 600–700 K, the step separation in different types of dislocations in NaCl vary from about 0.2 to 0.04 μm. In KCl λ is assumed to be of the same order of magnitude. Therefore, because the step separation decreases with increasing temperature, for our calculation in the case of KCl a value of 0.05 μm would be a reasonable estimation of this parameter, as its upper limit, at temperatures above 800 K. Hence the calculation results in $\alpha_d(900\ \text{K})/\alpha_d(800\ \text{K}) = 0.88$. In our previous study with KCl [17] we have obtained the ratio $\delta(900\ \text{K})/\delta(800\ \text{K}) = 0.75$. It follows that $\alpha_v(900\ \text{K})/\alpha_v(800\ \text{K}) < \alpha_d(900\ \text{K})/\alpha_d(800\ \text{K})$.[‡] Thus, in the KCl case we can conclude that the surface diffusion-related constraint, which is determined within a scope of the TLK model alone, apparently must take account of the other factors leading to a decrease of α_v. Presumably this conclusion is valid also for cesium iodide, though in contrast to the (001) surface of KCl the diffusion on the (011) CsI surface is not isotropic.

Next we consider the surface concentration of impurities. One expects a considerable enrichment of divalent cation impurities (Ba^{2+} is the most abundant in CsI) at the surface due to a lower fugacity of corresponding molecules, e.g. BaI_2. This would cause a decrease in the constraint parameter α_l due to the impeding action of impurity ions, which can be ascribed to a blocking of kink sites, because of a possible reduction of ion exchanges at these sites. However, the impurity effect is expected to be of greater significance at lower temperatures because at higher temperatures the competitive process of impurity diffusion into the bulk may proceed at a high rate thereby preventing the impurity accumulation at the surface [40]. In this way a decrease of the vaporization coefficient with decreasing temperature [low temperature part of $\delta(T)$ dependence in Fig. 3] is conceivable. Therefore, since the temperature dependencies of the parameters α_d and α_l may exhibit opposing tendencies one may suggest that the temperature dependence of their product $\alpha_l\alpha_d$ may pass through a maximum, thus providing a possible explanation for the origin of the maximum in Fig. 3. Another possible explanation, which we believe more plausible, refers to the point-defect-related constraint in the vaporization mechanism, i.e. the surface charge. Therefore, in what follows we focus on the possible changes in α_v with the temperature as predicted by the surface charge model.

[‡] Estimated values of λ less than 0.05 μm would result in greater values of the ratio $\delta(900\ \text{K})/\delta(800\ \text{K})$.

3.1.4. Surface charge model analysis

Surface charge can decrease the vaporization coefficient of alkali halides due to (1) a hindered rotation of molecules at the surface that would result in their slower diffusion from the ledges to the admolecule positions; and (2) an increase of the activation energy for molecule desorption owing to dipole interaction energy between the desorbing molecule and the charged crystal surface [3,17]. For example, the surface charge-related constraint, α_c, estimated by us [17] for a KCl crystal with the concentration of divalent metal impurity of 1 ppm equals to 0.99 and 0.92 at 800 and 900 K, respectively. Thus, with account of the two constraints, α_c and α_d, the ratio $\alpha_d(900\ \mathrm{K})\alpha_c(900\ \mathrm{K})/\alpha_d(800\ \mathrm{K})\alpha_c(800\ \mathrm{K}) = 0.82$ becomes closer to the previously mentioned experimental ratio $\delta(900\ \mathrm{K})/\delta(800\ \mathrm{K}) = 0.75$. Although we cannot make similar estimates of α_c for CsI because of the lack of data, still an application of the surface charge model in this case may be helpful for the interpretation of the results. This is mainly due to a material-specific way of variation with temperature of the properties of the electrical boundary layer in alkali halides. This variation is addressed briefly now (for more details see, e.g. [17]). Because the Gibbs free energy of formation of cation vacancies is less than that for anion vacancies, the surface has an intrinsic positive charge owing to the preferential formation of cation vacancies there. However, the presence of divalent cationic impurities in alkali halide crystals of nominal purity results in the occurrence of a negative extrinsic surface charge at sufficiently low temperatures when the concentration of extrinsic cation vacancies exceeds that of intrinsic ones. The crossover point at which the charge vanishes is the extrinsic isoelectric temperature (T_i), which is a function of both the impurity concentration and Gibbs energy for the formation of cation vacancies.

It follows that at the isoelectric temperature the surface charge-related constraint is eliminated. Therefore, if this temperature falls within the range studied, the $\alpha_v(T)$ dependence may pass through a maximum at this temperature, provided that the influence of surface charge on the vaporization kinetics is significant. Thus it can be suggested that the maximum of $\delta(T)$ dependence in Fig. 3 is due to the temperature variation in surface charge near T_i. The fact that the thermobalance data [20] do not exhibit a decrease in the vaporization coefficient at low temperatures, as it has been already mentioned, may be a consequence of a much lower sensitivity of that method with respect to the effect of surface charge on the vaporization rate. The point is that the fluxes leaving the crystal surface at different angles θ to the surface normal (more exactly, to the normal to surface cross section in case of rough surface) embody different information about this effect. In other words, the constraint of surface charge is operating with increasing power as the molecular velocity vector approaches the direction of the normal because the strength of surface charge field is supposed to be maximal in this direction. In mass-spectrometric methods, fluxes characterized by small θ are measured. According to estimations [18], only magnitudes of E roughly greater than $10^5\ \mathrm{V\ m^{-1}}$ can be of significance to experimental observations by the thermobalance method, i.e. at temperatures significantly higher than T_i. Moreover, on the assumption that the surface charge plays an increasing part in retardation of free-surface vaporization rate with increasing temperature, one can expect that also at high temperatures mass-spectrometric data would demonstrate a greater decrease in the vaporization coefficient than the thermobalance data can. Indeed, our results indicate that in going from $T = 700$ to 800 K, the decrease in δ (Fig. 3) is approximately 1.4 times greater than that in α_v (Fig. 4), as reported by Ewing and Stern for CsI [20].

On the other hand, in view of the results of theoretical work by Poeppel and Blakely [41] the validity of the surface charge model at high temperatures is open to argument. These authors have shown that surface charge may be largely reduced because of a limited number of surface sites (kinks) which can accommodate excess charge. Only for [41]

$$\sigma/e < 0.5N_s \tag{7}$$

(where σ is the surface charge density; e is the elementary charge; N_s is the number of surface kink sites per unit area) is the variation in surface electrical

properties in agreement with that predicted by defect theory with no account of possible deficiency of surface kinks. To check on whether the condition indicated by Eq. (7) holds in the intrinsic range in the case of alkali halides, the individual Gibbs energies for the formation of cation and anion vacancies must be known. To our knowledge, reliable experimental values of these energies are reported only for KCl [42]. Let us inspect this case. Intrinsic value of σ is defined [17]

$$\sigma = 2(2\epsilon\epsilon_0 nkT)^{1/2} \sinh(e\phi_s/2kT) \quad (8)$$

where ϵ is the dielectric coefficient; ϵ_0 is the permittivity of free space; ϕ_s is the surface electrical potential (which is defined as

$$\phi_s = (g^+ - g^-)/2e \quad (9)$$

with g^+ and g^- being the Gibbs free energy of formation of anion and cation vacancies, respectively) and n is the concentration of Schottky pairs in the bulk. The latter is determined by

$$n = N \exp(-g_s/2kT)/\gamma \quad (10)$$

where N is the number of lattice sites (cation and anion) per unit volume; g_S is the Gibbs free energy of formation of Schottky pairs; γ is the activity coefficient which can be specified from the Debye-Hückel-Lidiard theory [43]. The following parameters and approximating equations were used in calculation of σ: g^- (eV) = 1.256 − 4.53 kT [41]; g_s(eV) = 2.52 − 8.35 kT [44,45]; $\gamma = 1.18 - 3.77 \times 10^{-7}\ T^2$ [44]; $\epsilon = (2.14 + 4.21 \times 10^{-7}\ T^2)^2$ [46]; $N = 1.61 \times 10^{28}$ m^{-3} [37]. For example, in the temperature range 800–900 K of our investigation on KCl [17] the value σ/e is estimated to range from 3.1×10^{10} cm^{-2} through 9.7×10^{10} cm^{-2}. At T = 1050 K just below the melting point the upper limit of σ/e is 3.7×10^{11} cm^{-2}. On the other hand, considering the total number of surface sites on KCl, which amounts to approximately 1.0×10^{15} cm^{-2}, for a step separation of 50 nm, one may assume a maximum number of N_s of about 1.0×10^{12} cm^{-2}, taking the kink separation equal to the length of a chain of three ion pairs or to 1.57 nm. With this value of N_s the condition of Eq. (7) is met. However, because the Gibbs energy for kink formation is not known, one cannot exclude that the real concentration of kinks is significantly less than estimated above, and hence some reduction in surface charge occurs. This is as far as we can go with the inspection of Eq. (7) in the case of alkali halides. Alternatively, the evidence for the predicting power of the Poeppel and Blakely model can be gained from a comparison of the results on the direct measurements of surface electric potential and those yielded by defect theory. In this way, the measurements by a radiotracer technique [47,48] and subsequent theoretical analysis [49] of the subsurface electric potential in oriented single crystals of AgCl have not resulted in observation of the suppression in surface potential as predicted by Poeppel and Blakely for this salt. Unfortunately, no such results were reported for alkali halides because for several technical reasons (one must control the etching, and it must be possible to quench in the tracer distribution from the anneal temperature) it is more difficult to use this method on these salts.

Summing up, we can say that the surface charge model does not seem to lose its significance even at sufficiently high temperatures, though the possibility of some reduction in σ at high temperatures should be kept in mind.

The above reasoning can be helpful in interpreting the results of the work of Ewing and Stern [20], by re-examining Fig. 4. One can see in Fig. 4 that the vaporization rates of the solid and the liquid are equivalent when very close to the melting point and that the vaporization coefficient has a minimum value at the melting point. At this temperature the TLK model is no longer valid, whereas the surface charge concept, in our opinion, can still explain the observation. Although at first glance the point-defect-related constraint would be eliminated at the melting point, i.e. the electric boundary layer that exists at a solid surface due to defect formation processes would start to suffer disruption. Yet, this may not happen just at the melting point. The liquid retains some solid structure (and hence some surface stoichiometry) just above the melting point, as it was proposed by Ewing and Stern [20] on the basis of knowledge about the

continuity of solid and liquid states gained by Ubbelohde [50]. It is therefore conceivable that the rapid increase in the vaporization rate on heating the salt over 10–20 K above its melting point results from the melting of solidlike regions in the liquid. Namely in the course of such heating the surface stoichiometry inherent in the solid-state boundary layer disrupts totally (elimination of surface charge-related constraint), and the vaporization achieves its maximal rate, at which the vaporization coefficient equals approximately to unity (see Fig. 4). However, on further heating the free-surface vaporization rate again decreases significantly in comparison with the equilibrium rate. Such an effect may be presumably attributed to the reviving of the surface charge constraint because of formation of the electric boundary layer at the surface of a salt melt, as a liquid electrolyte.

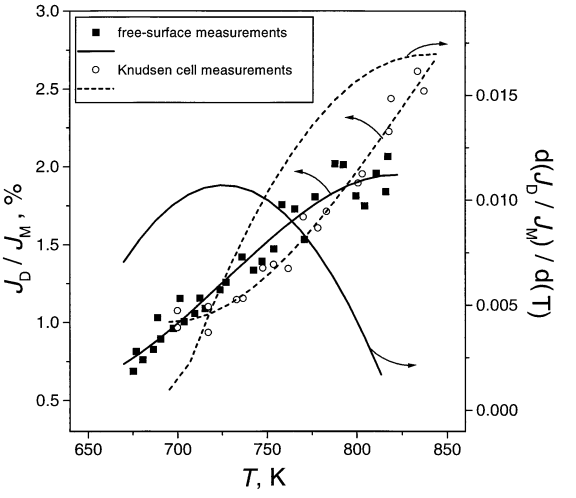

Fig. 5. Temperature dependence of dimer-to-monomer flux ratio and its derivative.

3.1.5. Dimer-to-monomer ratio

It was of interest to compare the temperature dependence of a dimer-to-monomer ratio, J_D/J_M, in the fluxes vaporized from an open CsI surface and effused from the Knudsen cell. The calculations were performed using the experimental currents of Cs^+, CsI^+, and Cs_2I^+ ions by

$$J_D/J_M = I(Cs_2I^+)\sigma_M/\sqrt{2}\sigma_D[I(Cs^+) + I(CsI^+)] \quad (11)$$

The ratio of the ionization cross sections, σ_D/σ_M, was set equal to 1.5 [51]. The results of the calculation are shown in Fig. 5, with best-fit lines approximating the data. One can see in Fig. 5 that there is no significant difference in the fraction of dimers between the free vaporization and equilibrium cases at each temperature. On the other hand, the important observation is that the shapes of the curve $J_D/J_M - T$ are somewhat different. To analyze the changes in the dimerization rate with the temperature, the derivatives, $d(J_D/J_M)/dT$, were calculated and are also shown in Fig. 5. It is well seen that in each case the values of $d(J_D/J_M)/dT$ vary with temperature in a different way. In the case of the Knudsen cell vaporization the ratio J_D/J_M increases with increasing temperature at a progressively increasing rate, whereas in the free-surface vaporization case the derivative passes through a distinct maximum.

The different shapes of the curve $d(J_D/J_M)/dT$ versus T may be the result of changes in the rate of association reactions with temperature and/or the difference in the temperature dependence of the constraints (rate-controlling factors) in the vaporization mechanisms of monomers and dimers. It has been inferred by Dabringhaus and Meyer [52] that at the alkali halide surfaces, the dimers are formed by collisions of ion pairs at the steps but not at the terraces (mechanism I) or broken off in one piece from kinks (mechanism II). The fact that the values of J_D/J_M obtained in this study for the cases of the free-surface and equilibrium vaporizations are in close agreement is an additional evidence for this inference. However, in the context of TLK model alone it is difficult to explain an origin of maximum on the curve $d(J_D/J_M)/dT$ versus T in the free-surface vaporization case. We propose that the taking into account the point-defect-related constraint, i.e. the likely influence of surface charge on the association kinetics and the vaporization mechanisms, can modify the TLK model in this case as well.

It is reasonable to assume that the maximum on the

curve $d(J_D/J_M)/dT$ versus T is formed in vicinity of T_i. Then it follows that the vaporization rate of the dimers is retarded by the surface charge to a greater extent than that of the monomers. We can propose the following reasons for the retardation. At the stage of dimer formation the retardation is possible if mechanism I is the operative process. In order to form a dimer molecule, one of the two colliding ion pairs has to reorient itself, as an electric dipole, to an energetically unfavorable position with respect to the field of the surface charge. Hence the dimerization rate is expected to pass through a maximum near the isoelectric temperature. Due to different electric polarizabilities, β, of monomers and dimers the retardation of the vaporization rate of dimers relative to monomers is also possible at the two final stages of the vaporization mechanism: surface diffusion and desorption. Obviously, the larger is the polarizability, the greater is the retardation because of the respective increase in the activation energies for diffusion and desorption. It has been found by Guella et al. [53], using a molecular beam electric deflection method, that dimers of alkali halides possess very large polarizabilities comparable to those of the alkali metal atoms. In particular, the mean value of β for Cs_2I_2 is determined to be 51.8×10^{-24} cm^3 [53], whereas for monomers the reported β equals to 9.8×10^{-24} cm^3 [54].

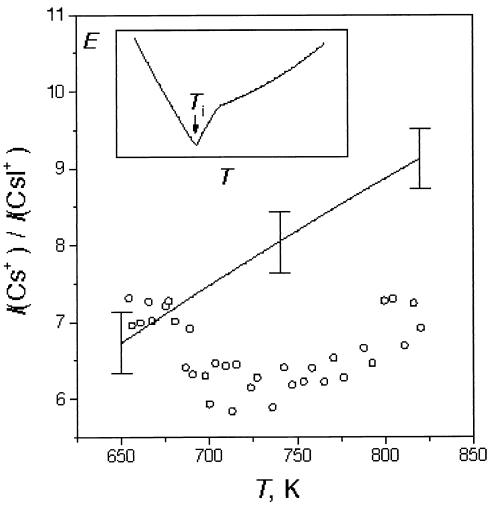

Fig. 6. Temperature dependence of the ion current ratio $I(Cs^+)/I(CsI^+)$ for the free-surface vaporization and for the Knudsen cell measurements (solid line; error bars indicate the datum scatter). Inset shows the way of variation in the strength of surface charge field with the temperature in the vicinity of T_i.

3.1.6. Electron-impact-fragmentation pattern

Another interesting observation of this work, which can possibly be related to the temperature dependence of the constraint parameter α_e, is the temperature dependence of the $I(Cs^+)/I(CsI^+)$ ratio. As illustrated in Fig. 6, the electron-impact-fragmentation patterns of CsI molecules for the cases of Knudsen cell effusion and free-surface vaporization are different. In the former case, this ratio increases roughly linearly with increasing temperature, whereas in the latter case it passes through a minimum. The occurrence of the minimum is open to speculation. It may be conjectured that this behavior is connected with a change in the Franck-Condon factors for ionization.

It is a matter of experience that the fragmentation pattern depends on both the vibrational and rotational excitation states of a molecule to be ionized and the internuclear distances in this molecule and its ion. The interplay of these parameters may yield both increasing and decreasing fraction of the fragment ions in a fragmentation pattern with a change in temperature. It has been demonstrated theoretically by Dronin and Gorokhov [55] with cesium chloride that with increasing temperature the increase in ion current ratio $I(Cs^+)/I(CsCl^+)$ may result from rotational excitation which is almost completely transferred from a molecule to an ion upon the ionization, and that the decrease in $I(Cs^+)/I(CsCl^+)$ may stem from the anharmonicity factor characteristic of a molecule to be ionized. However, in a narrow temperature interval these opposing tendencies can hardly become evident. In all probability the temperature factor alone may cause only unidirectional change in the fragmentation pattern. The nearly linear character of the temperature dependence of fragmentation pattern in the Knudsen cell measurements both with CsCl [22] and CsI supports this statement.

Therefore, in our opinion, the most likely speculation is that the passing of fragmentation pattern

through a minimum in the free-vaporization case is indicative of the action of surface-charge-related factor since apparently, with the exception of the surface temperature, no other surface-related factors can influence the state of vibrational and rotational excitation of a vaporizing molecule. The molecular energy shift, ΔW, due to an external field of the strength E is given by

$$\Delta W = -\beta E^2/2 \tag{12}$$

In the field of surface charge, whose strength can be predicted to vary from zero to the magnitudes of the order of 10^6 V m^{-1} in the vicinity of T_i [17], the energy shift of CsI molecule that possesses appreciable polarizability may exceed significantly (or be comparable to) the value of kT. For example, for the largest expected field strength, a ΔW value of 5×10^{-18} J is estimated, compared to a thermal energy of the order of 10^{-20} J. Therefore, the conversion of the energy ΔW to the energy of vibrational and/or rotational excitation when the subliming molecule leaves the surface would lead to a change in the electron-impact-fragmentation pattern, the ratio $I(Cs^+)/I(CsI^+)$ takes an extreme value at T_i when $E = 0$. This assumption is supported by a good correlation observed between the variation in fragmentation pattern with temperature in the free-surface vaporization case and the pattern of the curve E–T as predicted by defect theory [17] (see inset in Fig. 6). We have previously found such a correlation in the KCl [56] and KBr [18] cases.

Completing this line of reasoning, one can concede that the dimer molecules Cs_2I_2 in the vaporizing fluxes from an open crystal surface gain even greater vibrational excitation than the monomers because of their larger polarizability. Significantly different ratios of current intensities of Cs_2I^+ and Cs_2^+ ions—the products of electron-impact fragmentation of dimers—in the mass spectra recorded in the cases of the Knudsen cell and free-surface vaporization (see Secs. 3.1.1 and 3.1.2) can be considered as an indirect evidence for this assumption.

3.2. Ionic sublimation

In thermionic emission mass-spectra, Cs^+, Cs_2I^+, $Cs_3I_2^+$, and Cs_2^+ positive ions, and I^- and CsI_2^- negative ions were identified. The currents of negative ions were much weaker than those of positive ions. We were able to detect positive ions at temperatures higher than 600 K, whereas negative ions could be detected only above about 850 K. It is noteworthy that thermal ion currents were decreasing at the initial period of vaporization, as it was observed in the vaporization of KF [27], KCl [17], and KBr [28]. This decrease is obviously a reflection of the developing surface morphology which goes through the stage of formation of thermal etch pits. The deeper the pits, the less efficient the ion extraction is and thus the weaker the thermal ion current measured [27].

Undoubtedly, the ions emitted play a minor part in mass transfer from the surface in comparison with the molecules vaporized. It is a matter of experience that the saturation flux of thermal ions, $J^{\pm}$, that can be extracted from unit area of ionic solid per unit time is several orders of magnitude smaller than the molecular flux J. For illustration, such a comparison can be made, for example, in the case of KBr for which both the electrometric [28] and thermobalance [20] measurements have been carried out. At $T = 800$ K positive thermionic emission from polycrystalline samples of this salt is characterized by a current density of the order of 10^{-9} A cm^{-2} [28]; that is $J^+ = 6 \times 10^9$ cm^{-2} s^{-1}. The flux J from KBr single crystal at this temperature is found to be about 4×10^{16} cm^{-2} s^{-1} [20]. Also, the surface concentration of the adions is naturally expected to be significantly smaller than that of the admolecules. This is mainly conditioned by the difference in the binding energy of molecules and ions to the kink sites. On the other hand, it is clear that thermal ion emission is expected to reflect the electrical surface properties with much greater response than the sublimation of neutral molecules. For example, the activation energy for cation/anion sublimation from the charged surface is given as [27]

$$E_s = E_M - 0.5e|\phi_p| \pm e|\phi_s| \tag{13}$$

where E_M is the Madelung energy; ϕ_p is the polarization potential. In the extrinsic temperature range the surface electrical potential, ϕ_s, is defined [17]

$$\phi_s = -(g^- + kT \ln \alpha)/e \quad (14)$$

where α is the mole fraction of divalent metal impurities. In the intrinsic range ϕ_s is given by Eq. (9).

By way of example, let us consider the case of positive ion emission. Then the signs "+" and "−" in the third term in Eq. (13) refer, respectively, to the extrinsic (the value of ϕ_s is negative) and intrinsic (the value of ϕ_s is positive) ranges. The Gibbs energy of defect formation is defined as

$$g^{\pm} = h^{\pm} - Ts^{\pm} \quad (15)$$

where $h^{\pm}$ and $s^{\pm}$ are the enthalpy and the entropy of formation of anion/cation vacancies, respectively. Thus, from Eqs. (9), (14), and (15), Eq. (13) becomes

$$E_s = E_M - 0.5e|\phi_p| + h^- + T(k \ln \alpha - s^-) \quad (16)$$

$$E_s = E_M - 0.5e|\phi_p| - [h^+ - h^- + T(s^- - s^+)]/2 \quad (17)$$

for the extrinsic and intrinsic ranges, respectively. Since thermal ion current is proportional to the exponential factor $\exp(-E_s/kT)$, the break of an experimental curve $\ln I - 1/T$ is expected to be observed in going from the extrinsic range to the intrinsic one. The break-point temperature is likely to correspond to so-called "knee temperature," T_k, which is somewhat higher than T_i and is given theoretically by

$$T_k = -g_S/2k \ln \alpha \quad (18)$$

Note that if we neglect the temperature dependence of E_M and ϕ_p, from Eqs. (16) and (17), then the difference in the apparent activation energies for ion sublimation, derived from the slopes of the curve $\ln I - 1/T$ above and below T_k, would be equal to $h_S/2$, where $h_S = h^+ + h^-$ is the enthalpy of formation of Schottky pairs. So the break of a curve is assumed to be quite distinct.

To provide experimental support for the above mentioned reasoning, the temperature dependence of thermal ion current has to be measured over an interval covering both extrinsic and intrinsic ranges. From this point of view, only the current of Cs^+ ions was intense enough to be measured at temperatures sufficiently low to fall within the extrinsic range. Such a temperature dependence that incorporates the data of successive cooling and heating runs is shown in Fig. 7. It should be noted that these measurements were carried out after the sample had been heated to 820 K in order to accelerate the development of surface topography. Once the isothermal ion current had achieved reproducibility to within 10% in half an hour, the readings were taken. In accordance with expectations, the experimental curve shown in Fig. 7 reveals a break at $T_k = 730 \pm 10$ K. The activation energies for sublimation of Cs^+ ions are determined to be 2.16 ± 0.10 and 1.79 ± 0.05 eV from the slopes of the curve portions below and above the break-point temperature, respectively. To the best of our knowledge, a reliable value of h_S for cesium iodide has not been reported; the available values are widely scattered and fall in the range of 1.1–2.25 eV [57]. Nevertheless, it is safe to assume that $h_S/2 \geq 0.55$ eV. The difference in the experimental magnitudes of E_s, equal to 0.37 ± 0.11 eV, is less than this

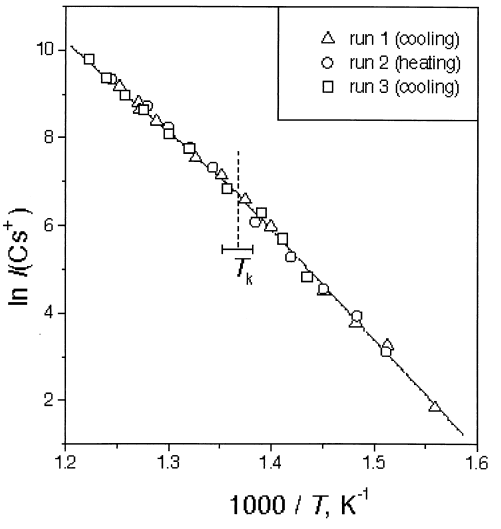

Fig. 7. Temperature dependence of the thermal emission current (arbitrary units) of Cs^+ ions.

Table 1
Thermionic emission mass spectra

	Relative intensities of ion current							
T(K)	Cs^+	Cs_2^+	Cs_2I^+	$Cs_3I_2^+$	I^-	CsI_2^-	$Cs_2I_3^-$	
877	100	0.30	19.8	0.07	0.025	0.10	···	Free-surface measurements[a]
837	35.7	···	100	0.52	19.1	47.8	3.5	Knudsen cell measurements[b]

[a] This work.
[b] See [29,30].

value. So it is likely that the values of E_M and ϕ_p, being temperature dependent as well, also contribute to the difference in the magnitudes of E_s. Also, one should take into account the deficiencies of the plane surface model [Eqs. (9) and (14)] in describing the electrical properties of rough surfaces.

Further discussion will focus in the thermionic emission mass-spectra. Relative current intensities of ions of both signs, exemplified at $T = 877$ K, are listed in Table 1 along with the Knudsen cell mass-spectrometric data [29,30][§] on ions that exist in the saturated vapor over CsI. The analysis of the data in Table 1 allows the following conclusions to be made: (1) thermal currents of negative ions emitted from the Knudsen cell are nearly equal in intensity with those of positive ions, whereas the free crystal surface emits positive ions in much greater amount than negative ions and (2) in contrast to the electron-impact-ionization mass-spectra case, thermionic emission mass spectra obtained in this work differ markedly from those in the Knudsen cell measurements [29,30]. Specifically, the fraction of Cs_2I^+ and $Cs_3I_2^+$ cluster ions decreases drastically relative to Cs^+ ions in the case of free vaporization, whereas the fraction of CsI_2^- ions relative to I^- ions becomes even greater.

We suppose that the difference in relative emission efficiency of positive and negative ions under equilibrium and nonequilibrium conditions may be due to nonstoichiometry in kink-site occupancy by cations and anions, favoring the emission of positive ions from a freely vaporized surface [27], and/or different binding energies of cations and anions at the kink sites of a charged ledge. Indeed, since we compare the emission efficiencies in the intrinsic range, i.e. in the case of positive ledge charge, the kink binding energy of cations is expected to be smaller than that of anions. Besides, the reduction in the number of anion kinks is expected because of their blocking by the impurity cations.

The following can be offered as an explanation for the difference in the mass spectra mentioned previously. Most likely the cluster ions are formed by the surface reactions of the types

$$Cs^+ + CsI \Rightarrow Cs_2I^+ \quad (19)$$

$$Cs^+ + Cs_2I_2 \Rightarrow Cs_3I_2^+ \quad (20)$$

$$I^- + CsI \Rightarrow CsI_2^- \quad (21)$$

$$I^- + Cs_2I_2 \Rightarrow Cs_2I_3^- \quad (22)$$

One can also consider that these clusters can form by breaking off in one piece from the kink sites. However, this mechanism seems less plausible since neither the TLK model nor the surface charge concept implies a change in the ratio of the ion currents Cs_2I^+/Cs^+ or CsI_2^-/I^- in going from equilibrium to nonequilibrium conditions. So we can exclude this mechanism from further consideration. Most probably that the ion clusters, like molecular dimers, are formed at the steps, and obviously the outcome of the reactions indicated in Eqs. (19)–(22) would depend on the near-step concentrations of neutral and charged

[§] The measurements of thermionic emission mass spectrum of CsI reported in [29] were repeated later by Sidorova [30] (not published) with a new design of ion source providing higher detection sensitivity and eliminating the current fluctuations observed in the previous study [29]. Nonetheless the mass spectrum itself and the relative intensities of ion currents are essentially identical in both studies.

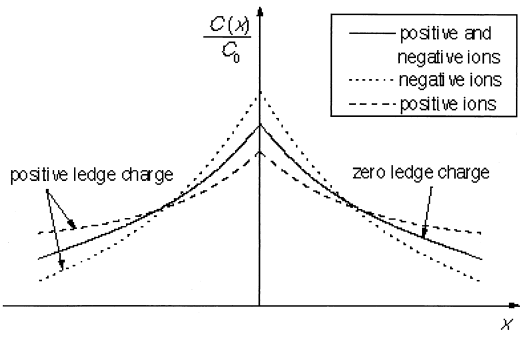

Fig. 8. Normalized adion concentration as function of the distance from a ledge.

particles. Here it is pertinent to note that an additional feature not predicted by the planar surface charge model is a substantial nonuniformity of surface charge. The excess surface charge is located predominantly at the steps resulting from the excess number of kinks of one sign. Harris and Fiasson [58] obtained experimental verification of this statement by scanning across as-cleaved surfaces of NaCl by a vibrating capacitor probe. They found that maximum surface potential coincided with location of cleavage steps. Thus, at the step location the vector of the strength of surface charge field would have an appreciable projection onto the axis perpendicular both to the surface normal and to the step. Therefore, the near-step and terrace concentrations of adions would strongly depend on the ledge (step) charge. The assumed near-ledge distribution of adions of opposite sign in the cases of zero and positive ledge charge, as an appropriate example, is illustrated in Fig. 8, as a function $C(x)/C_0$ versus x, where $C(x)$ is the concentration of adions of given kind at a distance x from a ledge; C_0 is the total concentration of these adions on a terrace. One can see in Fig. 8 that in the case of a positively charged ledge the concentration of positive ions, located readily at the step, increases in comparison with that in the case of uncharged ledge, whereas the concentration of negative ions decreases. On the other hand, in the case of Knudsen cell measurements it is safe to assume that there is no difference in the near-step concentration of adions of both signs because there is no electric field of surface charge in the inner space of an enclosure.

The measurements of the currents of cluster ions were performed in the intrinsic temperature range. In this range, Cs^+ ions are repelled off the positively charged ledge and hence their concentration at a step is reduced. Therefore, the probability of formation of Cs_2I^+ and $Cs_3I_2^+$ cluster ions at freely vaporized surfaces by the reactions of Eqs. (19) and (20), respectively, is expected to be much smaller than under the equilibrium conditions, as it was experimentally observed. On the other hand, in the case of negative ions, coulombic interactions of I^- ions with the positively charged ledge brings them closer to the ledges, thereby increasing their concentration at a step and hence the probability of formation of CsI_2^- ions by the surface reaction of Eq. (21).

The mechanism of formation of Cs_2^+ ions at freely vaporized surfaces is a challenging question. It may proceed through the dissociation of Cs_2I^+ ions. However, if this were the case, Cs_2^+ ions would be emitted from the Knudsen cell also. Since Sidorova et al. [29,30] have not observed these ions in thermionic emission mass spectra from the Knudsen cell, we propose the following alternate mechanism of their formation that relates to the local irregularities of surface charge field. The speculation is that the non-uniform character of surface charge may promote the formation of F centers (iodine vacancies in which electrons are trapped) and iodine atoms. The combination of F centers with Cs^+ ions results in the formation of cesium atoms. The latter react with Cs^+ ions to yield Cs_2^+ ions. Presumably, such a nonequilibrium process does not occur inside the Knudsen cell.

For comparison purposes, the activation energies for sublimation of Cs^+, Cs_2I^+, and Cs_2^+ ions have been determined in separate measurements. In order for such measurements to be made, the crystal was initially overheated at $T = 890$ K for about 10 min to allow for the development of surface structure at a relatively high rate. Then the ion currents were recorded throughout cooling and heating procedures in the temperature range 750–890 K. These data are shown in Fig. 9 as the natural logarithm of the ion

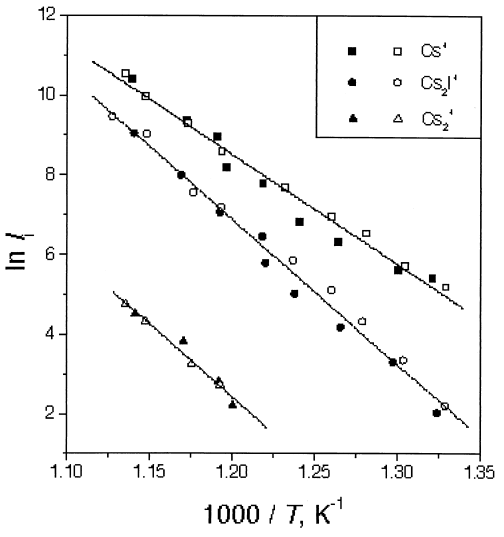

Fig. 9. Temperature dependence of the thermal emission current (arbitrary units) of Cs^+, Cs_2I^+, and Cs_2^+ ions. Closed and open symbols correspond to the heating and cooling runs, respectively.

current intensity plotted against reciprocal temperature. Linear fit yielded values of E_s as follows: 2.37 ± 0.09 eV (Cs^+), 3.13 ± 0.09 eV (Cs_2I^+), and 3.15 ± 0.21 eV (Cs_2^+). Thus within the experimental errors an equal energy is required to remove Cs_2I^+ or Cs_2^+ ions, whereas the removal of Cs^+ ions requires significantly less energy.

4. Conclusions

The thermodynamics and kinetics of the vaporization of cesium iodide single crystal are investigated by mass spectrometry. It is shown that this crystal vaporizes to give CsI and Cs_2I_2 molecules under both conditions of equilibrium and free-surface vaporization. The analysis of the temperature dependencies of ion currents in the case of free-surface vaporization provided the temperature dependence of the vaporization coefficient of both monomers and dimers due to the combined effect of factors related to surface structural roughening, impurity segregation, and electric boundary layer. The dimer-to-monomer ratio is found to increase with temperature at a continually increasing rate in the case of the Knudsen cell measurements, and at a rate passing through a maximum in the case of free-surface vaporization. The surface charge of defect-related origin is proposed as an explanation for this kinetic effect.

It is observed that the temperature dependence of the electron-impact-fragmentation pattern of CsI molecules is roughly linear in the case of the Knudsen cell measurements but passes through a minimum in the case of free-surface measurements. It is concluded that molecules desorbing from an open crystal surface may possess excessive vibrational and rotational energy compared to that characteristic of thermal excitation.

It is found that the heated surface of a CsI crystal emits both positive and negative ions: Cs^+, Cs_2I^+, Cs_2^+, I^-, and CsI_2^-. The currents of negative ions are much weaker than those of positive ions. The temperature dependence of the Cs^+ ion current reveals a break that is attributed to the polarity reversal of the surface charge. In contrast to electron-impact-ionization mass spectra, thermionic emission mass spectra obtained in this work differ significantly from those measured in Knudsen cell mass-spectrometric studies.

References

[1] G.M. Rosenblatt, in Treatise on Solid State Chemistry, Surfaces I Vol. 6A, N.B. Hannay (Ed.), Plenum, New York, 1976, pp. 165–239.
[2] W.K. Burton, N. Cabrera, F.C. Frank, Philos. Trans. R. Soc. London, Ser. A 243 (1951) 299.
[3] D.W. Short, R.A. Rapp, J.P. Hirth, J. Chem. Phys. 57 (1972) 1381.
[4] J.E. McVicker, R.A. Rapp, J.P. Hirth, J. Chem. Phys. 63 (1975) 2645.
[5] Z.A. Munir, J.P. Hirth, J. Electron. Mater. 6 (1977) 409.
[6] I.V. Samarasekera, Z.A. Munir, High Temp. Sci. 10 (1978) 155.
[7] R.H. Wagoner, J.P. Hirth, J. Chem. Phys. 67 (1977) 3074.
[8] S.T. Lam, Z.A. Munir, J. Cryst. Growth 47 (1979) 373; High Temp. Sci. 12 (1980) 249; J. Cryst. Growth 51 (1981) 227.
[9] L.S. Seacrist, Z.A. Munir, High Temp. Sci. 3 (1971) 340.
[10] R.B. Leonard, A.W. Searcy, J. Appl. Phys. 42 (1971) 4047.
[11] G.A. Somorjai, J.E. Lester, J. Chem. Phys. 43 (1965) 1450.
[12] J.E. Lester, G.A. Somorjai, J. Chem. Phys. 49 (1968) 2940.
[13] Z.A. Munir, T.T. Nguyen, Philos. Mag. A 47 (1983) 105.
[14] Z.A. Munir, Res. Mech. 11 (1984) 1.
[15] Z.A. Munir, A.A. Yeh, Philos. Mag. A 56 (1987) 63.

[16] Z.A. Munir, J.P. Hirth, J. Appl. Phys. 41 (1970) 2697.
[17] M.F. Butman, A.A. Smirnov, L.S. Kudin, Appl. Surf. Sci. 126 (1998) 185.
[18] M.F. Butman, A.A. Smirnov, L.S. Kudin, Z.A. Munir, High Temp. Sci., in press.
[19] J.E. Lester, G.A. Somorjai, J. Chem. Phys. 49 (1968) 2940.
[20] C.T. Ewing, K.H. Stern, J. Phys. Chem. 79 (1975) 2007.
[21] G.M. Rothberg, M. Eisenstadt, P. Kusch, J. Chem. Phys. 30 (1959) 517.
[22] P.A. Akishin, L.N. Gorokhov, L.N. Sidorov, Dokl. Akad. Nauk SSSR 135 (1960) 113 (English translation: p. 1001 of Phys. Chem. Soc. 1960).
[23] L.N. Gorokhov, Thesis of Doctor of Chemistry, Moscow University, 1972.
[24] R. Viswanathan, K. Hilpert, Ber. Bunsenges. Phys. Chem. 88 (1984) 125.
[25] O. Gotzmann, P. Hoffman, F. Trummler, J. Nucl. Mater. 52 (1974) 33.
[26] Proceedings of Seminar on Iodine Removal from Gaseous Effluents in the Nuclear Industry, Commission of European Communities, Mol, Belgium, 21–24 September 1981.
[27] M.F. Butman, J. Nakamura, H. Kawano, Appl. Surf Sci. 78 (1994) 421.
[28] M.F. Butman, J. Nakamura, S. Kamidoi, H. Kawano, Appl. Surf. Sci. 89 (1995) 323.
[29] I.V. Sidorova, A.V. Gusarov, L.N. Gorokhov, Int. J. Mass Spectrom. Ion Phys. 31 (1979) 367.
[30] I.V. Sidorova, Thesis of Candidate of Physics and Mathematics, Institute for High Temperatures of Russian Academy of Science, Moscow, 1994.
[31] P. Winchell, Nature 206 (1965) 1252.
[32] H.H. Emons, W. Horlbeck, D. Kiessling, Z. Anorg. Allg. Chem. 488 (1982) 212.
[33] Z.A. Munir, J. Mater. Sci. 22 (1987) 2221.
[34] J.E. Lester, Ph.D. thesis, University of California, Berkeley, UCRL-17794, November, 1967.
[35] H.J. Meyer, H. Dabringhaus, in: Current Topics in Materials Science, Vol. 1, E. Kaldis (Ed.), North-Holland, Amsterdam, 1978, pp. 47–78.
[36] H. Frey, H.J. Meyer, J. Cryst. Growth 82 (1987) 435.
[37] Handbook of Chemistry and Physics, 64th ed. CRC Press, Boca Raton, FL, 1983–1984.
[38] Z.A. Munir, E.K. Chieh, J.P. Hirth, J. Cryst. Growth 63 (1983) 244.
[39] H. Dabringhaus, H.J. Meyer, Surf. Sci. 177 (1986) 451.
[40] J.T. Kummer, J.D. Youngs, J. Phys. Chem. 67 (1963) 107.
[41] R.B. Poeppel, J.M. Blakely, Surf. Sci. 15 (1969) 507.
[42] J.L. Tallon, R.G. Buckley, M.P. Staines, W.H. Robinson, Philos. Mag. 51 (1985) 635.
[43] F. Beniere, in Physics of Electrolytes, Academic, London, 1972, p. 203.
[44] M. Beniere, M. Chemla, F. Beniere, J. Phys. Chem. Solids 37 (1976) 525.
[45] L.A. Acuna, P.W.M. Jacobs, J. Phys. Chem. Solids 41 (1980) 595.
[46] P.W.M. Jacobs, J. Chem. Soc. Faraday Trans. 2 85 (1989) 415.
[47] R.A. Hudson, G.C. Farlow, L.M. Slifkin, Crys. Latt. Def. Amorph. Mat. 15 (1987) 239.
[48] R.A. Hudson, G.C. Farlow, L.M. Slifkin, Phys. Rev. B 36 (1987) 4651.
[49] K. Wonnell, L.M. Slifkin, Phys. Rev. B 48 (1993) 78.
[50] A.R. Ubbelohde, J. Chem. Phys. 61 (1964) 58.
[51] V.P. Glushko, Termodinamicheskie Svoistva Individual'nykh Veshchestv (Thermodynamic Properties of Individual Substances), Vols. 1–4, Nauka, Moscow, 1978–1984.
[52] H. Dabringhaus, H.J. Meyer, J. Cryst. Growth 40 (1977) 139; 61 (1983) 91; 61 (1983) 95.
[53] T. Guella, T.M. Miller, J.A.D. Stockdale, B. Bederson, L. Vuscovic, J. Chem. Phys. 94 (1991) 6857.
[54] S.P. Konovalov, V.G. Solomonic, Zh. Strukt. Khim. (Rus. J. Struct. Chem.) 23 (1982) 90.
[55] A.A. Dronin, L.N. Gorokhov, Teplophizika Vysokikh Temperatur (Rus. High Temp.) 10 (1972) 49.
[56] M.F. Butman, A.A. Smirnov, L.S. Kudin, Z.A. Munir, Int. J. Mass Spectrometry (1999) in press.
[57] M.N. Magomedov, Zh. Fiz. Khim. (Rus. J. Phys. Chem.) 67 (1993) 661.
[58] L.B. Harris, J. Fiasson, J. Phys. C: Solid State Phys. 18 (1985) 4845.